Insight Bulletin: A Multidisciplinary Interlink International Research Journal
Peer Reviewed International, Open Access Journal.
ISSN : 3065-7857 / Website: https://ibrj.us / Volume-3, Issue-5 / May - 2026

Original Article

AutoDock-Based Molecular Docking Analysis of Calcite–Carbonic Anhydrase Interactions: Mechanistic Insights for Enzyme-Mediated Biomineralization in Recycled Aggregate Concrete

Mrunal Date
Tuljaram Chaturchand College of Arts, Science and Commerce, Baramati

Manuscript ID:
IBMIIRJ -2026-030544

Submitted: 18 Apr. 2026
Revised: 26 Apr. 2026
Accepted: 15 May 2026
Published: 31 May 2026

ISSN: 3065-7857
Volume-3
Issue-5
Pp. 226-234
May 2026

Correspondence Address:
Mrunal Date
Tuljaram Chaturchand College of Arts, Science and Commerce, Baramati
Email: mrunaldate606@gmail.com

OPEN ACCESS

Quick Response Code:

Web. https://ibrj.us

DOI: 10.5281/zenodo.22122579

DOI Link:
https://doi.org/10.5281/zenodo.22122579

Creative Commons

Abstract

Enzyme-mediated biomineralization is increasingly recognized as a viable strategy for enhancing the microstructural integrity of recycled aggregate concrete (RAC). In this study, we report an in silico molecular docking investigation of the non-covalent interaction between calcite ($CaCO_3$)—the thermodynamically stable polymorph of calcium carbonate—and carbonic anhydrase (CA; EC 4.2.1.1), a zinc metalloenzyme central to biogenic carbonate precipitation. Docking simulations were performed using AutoDock 4.2 with the Lamarckian Genetic Algorithm (LGA). The top-ranked binding pose yielded a free energy of binding of −6.4 kcal/mol, corresponding to an estimated inhibition constant (K_i) of approximately 18.8 μM, indicative of a moderate-to-strong, thermodynamically favorable non-covalent interaction. Interaction analysis identified hydrogen bonding, electrostatic complementarity, and van der Waals contacts at the calcite–enzyme interface as primary stabilizing forces. These findings mechanistically support the role of carbonic anhydrase in nucleating calcium carbonate deposition within the pore network of RAC matrices. Critically, this work focuses exclusively on the computational characterization of the calcite–CA molecular interaction. Experimental validation through isothermal titration calorimetry (ITC), surface plasmon resonance (SPR), and microscale thermophoresis (MST), as well as the incorporation of biopolymeric and nanomaterial modifiers, are identified as high-priority future directions. The results establish a rigorous computational foundation for rationally designing enzyme-augmented, self-healing concrete composites in sustainable construction applications.

Keywords: *Molecular docking; AutoDock 4.2; carbonic anhydrase; calcite; biomineralization; recycled aggregate concrete; sustainable construction; free energy of binding; Lamarckian Genetic Algorithm; computational materials science.*

Introduction

The global construction sector generates an estimated 2–3 billion tonnes of construction and demolition waste annually, driving an urgent need for circular-economy approaches in building materials [1]. Recycled Aggregate Concrete (RAC), produced by substituting natural coarse aggregates with crushed construction and demolition debris, represents one of the most scalable pathways toward reducing waste landfilling and conserving virgin aggregate resources [2]. Despite its environmental appeal, RAC consistently exhibits lower compressive strength, higher water absorption, and reduced durability compared with conventional concrete—deficiencies primarily attributed to a mechanically inferior and porous Interfacial Transition Zone (ITZ) enveloping the recycled aggregate particles [3]. Biomineralization strategies, which harness the metabolic activity of microorganisms or the catalytic specificity of enzymes to precipitate inorganic minerals, have emerged as effective routes to improving concrete durability [4,5]. Among enzymatic approaches, carbonic anhydrase (CA; EC 4.2.1.1) has attracted considerable attention because it catalyzes the reversible hydration of carbon dioxide—$CO_2 + H_2O \rightleftharpoons HCO_3^- + H^+$—at rates approaching 10^6 s^{-1}, making it one of the fastest known enzymes [6]. In an alkaline concrete pore-solution environment rich in Ca^{2+} ions, the bicarbonate generated by CA-catalyzed CO_2 hydration can react rapidly to precipitate calcite ($CaCO_3$), the thermodynamically stable polymorph of calcium carbonate under ambient conditions [7].

How to cite this article:
Date, M. (2026). AutoDock-Based Molecular Docking Analysis of Calcite–Carbonic Anhydrase Interactions: Mechanistic Insights for Enzyme-Mediated Biomineralization in Recycled Aggregate Concrete. InSight Bulletin: A Multidisciplinary Interlink International Research Journal, 3(5), 226–234. https://doi.org/10.5281/zenodo.22122579

Calcite deposition within the pore network densifies the cementitious matrix, reduces water permeability, and potentially heals micro-cracks—effects that are especially desirable in the more porous ITZ of RAC [8]. While field- and laboratory-scale studies have demonstrated macroscopic improvement in RAC performance following bacterial or enzyme treatments [9,10], the molecular-scale mechanism by which CA interacts with, and potentially nucleates, calcite remains poorly characterized. Understanding the specific non-covalent interactions at the enzyme–mineral interface is prerequisite to the rational engineering of more active or stable CA variants and to the design of bio-inspired composite materials. Computational molecular docking provides a rapid, cost-effective, and reproducible means of probing such interactions at atomic resolution [11]. AutoDock 4.2, employing the Lamarckian Genetic Algorithm (LGA) for conformational search, is among the most widely validated docking platforms for ligand–protein binding prediction and has been extended to mineral surface interactions in recent literature [12,13]. In the present work, AutoDock 4.2 was deployed to simulate the binding of a modified calcite molecular cluster to the crystallographic structure of human carbonic anhydrase II (PDB: 3KS3). The study delivers quantitative thermodynamic parameters (ΔG^{bend}, K_i) and a qualitative interaction map for the calcite–CA complex, providing mechanistic underpinning for enzyme-mediated calcite precipitation in RAC pore environments. Importantly, this investigation is computational in scope; the paper explicitly delineates experimental validation as a future priority and does not extrapolate docking predictions to macroscopic concrete performance.

Objectives

The specific objectives of this computational study are:

1. To prepare crystallographically validated molecular structures of calcite and carbonic anhydrase for AutoDock-compatible docking simulations.
2. To determine the binding free energy (ΔG^{bend}) and estimate the inhibition constant (K_i) as thermodynamic descriptors of interaction strength.
3. To characterize the non-covalent interaction landscape—including hydrogen bonds, electrostatic contacts, and van der Waals interactions—at the calcite–CA interface.
4. To interpret the mechanistic implications of the docking results for carbonic anhydrase-mediated calcite nucleation in RAC pore environments.
5. To explicitly define the boundaries of this study and articulate a scientifically motivated roadmap for subsequent experimental and computational investigations.

Materials And Methods

1. **Receptor Preparation: Carbonic Anhydrase (PDB: 3KS3)**

The three-dimensional crystal structure of human carbonic anhydrase II in complex with a sulfonamide inhibitor was obtained from the RCSB Protein Data Bank (PDB entry 3KS3; resolution: 1.10 Å). The structure was pre-processed using Discovery Studio Visualizer (Dassault Systèmes Biovia) in which all heteroatoms, crystallographic water molecules and co-crystallized ligands were removed, hydrogen atoms were added at physiological pH (7.4) with the CHARMm force field and partial atomic charges were assigned using the Gasteiger–Marsili method. The catalytic zinc ion (Zn^{2+}) coordinated to His94, His96 and His119 stayed in the active site. The prepared receptor file was saved in PDBQT format for docking. The ribbon diagram of the prepared carbonic anhydrase structure in Discovery Studio is shown in Figure 1.

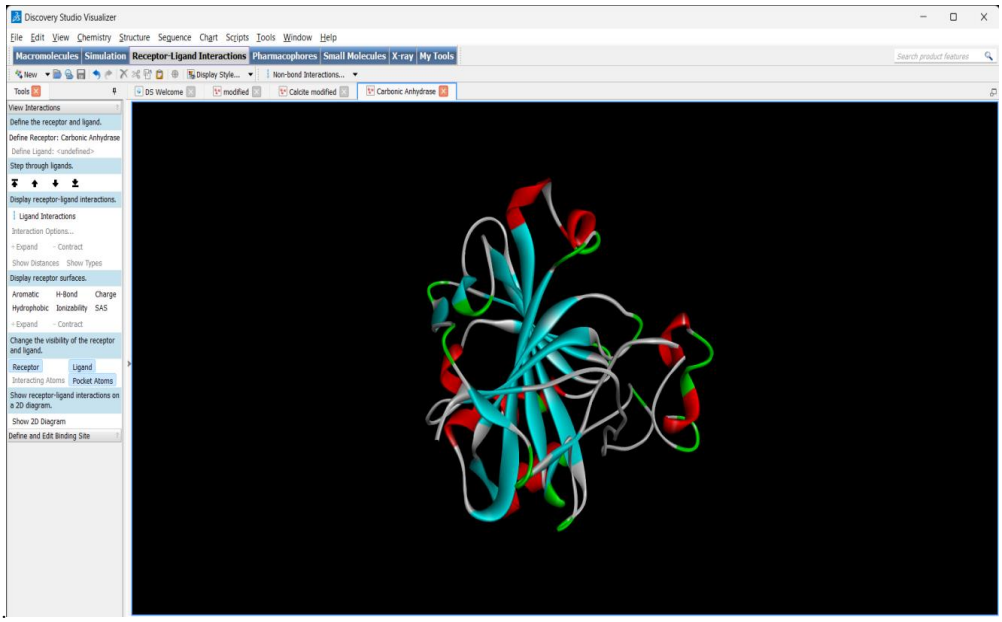

Figure 1. *Three-dimensional ribbon structure of carbonic anhydrase (PDB: 3KS3) prepared in Discovery Studio Visualizer. The β-sheet core (cyan), α-helical elements (red), and loop regions (grey) are rendered in secondary-structure coloring. The catalytic zinc center is locatedat the base of the central β-barrel.*

2. **Ligand Preparation: Modified Calcite Cluster**

A representative molecular cluster of calcites $CaCO_3$ was built in the typical crystallographic settings (space group R3c; a = 4.99 \AA, c = 17.06 \AA). Then the cluster was modified to include partial charges reflecting the electrostatics environment observed

at the calcite surface in the presence of water, according to the procedure proposed by Raiteri and Gale [14]. Then geometry optimization was performed at the semi-empirical PM7 level with MOPAC2016. After the optimized shape was ready, it was imported into Discovery Studio Visualizer, where hydrogen bond donors and hydrogen bond acceptors were identified and the final ligand was exported to PDBQT format as needed for AutoDock. Figure 2: The prepared calcite ligand in ball-and-stickview.

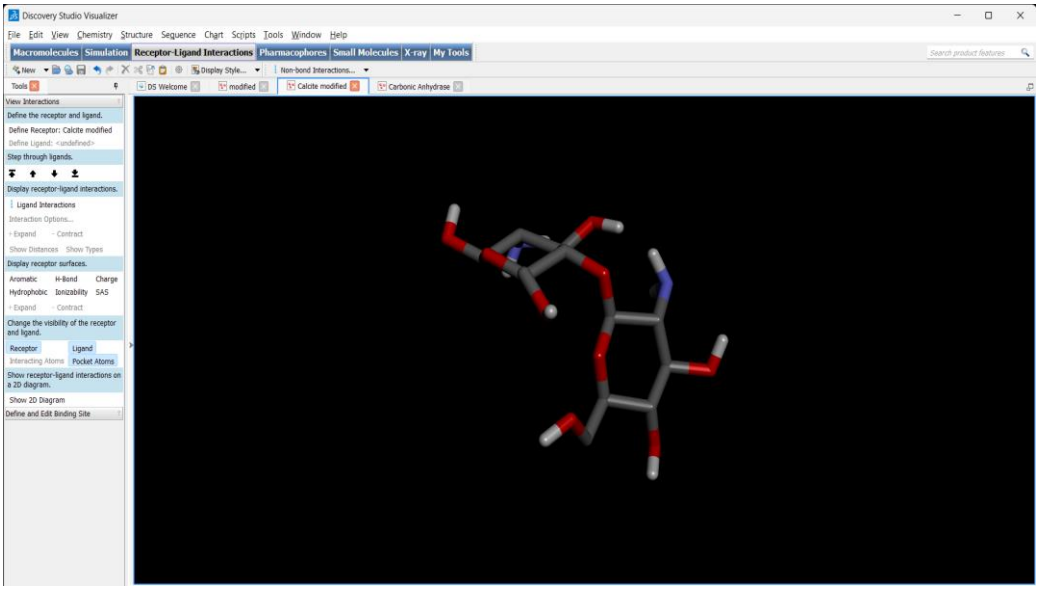

Figure 2. *Ball-and-stick model of the modified calcite ($CaCO_3$) molecular cluster prepared for docking. Carbon atoms are shown in dark grey, oxygen atoms in red, calcium atoms in grey-white, and coordinating nitrogen atoms (from carbonate analogue) in blue. The structure was geometry-optimized at the PM7 level prior to docking.*

3. Molecular Docking Protocol (AutoDock 4.2 / PyRx)

We used AutoDock 4.2 for molecular docking, running everything through the PyRx 0.8 interface. The receptor stayed rigid, while the calcite cluster acted as the flexible ligand. We set up a grid box measuring 60 by 60 by 60 Å, with points spaced 0.375 Å apart, centered right on the active-site zinc ion of CA—making sure the whole substrate-binding cleft was included. The docking relied on the Lamarckian Genetic Algorithm. Here's the setup: population size of 150, up to 2,500,000 energy evaluations, 27,000 generations, a mutation rate of 0.02, and a crossover rate of 0.80. We ran the docking nine times independently. Then we clustered all the resulting binding poses using a 2.0 Å RMSD cutoff. From all these, the pose with the lowest free energy of binding was picked as the top-ranked result. You'll find all the parameters and software details in Table 1.

Table 1. AutoDock 4.2 Docking Parameters

Parameter	Value
Software	AutoDock 4.2 via PyRx 0.8
Algorithm	Lamarckian Genetic Algorithm (LGA)
Population size	150
Max energy evaluations	2,500,000
Max generations	27,000
Mutation rate	0.02
Crossover rate	0.80
Number of docking runs	9
Grid box (x × y × z)	60 Å × 60 Å × 60 Å (0.375 Å/point)
RMSD clustering tolerance	2.0 Å
Receptor flexibility	Rigid
Ligand flexibility	Flexible (all rotatable bonds)

Table 1. Molecular docking parameters applied in AutoDock 4.2 via the PyRx virtual screening platform.

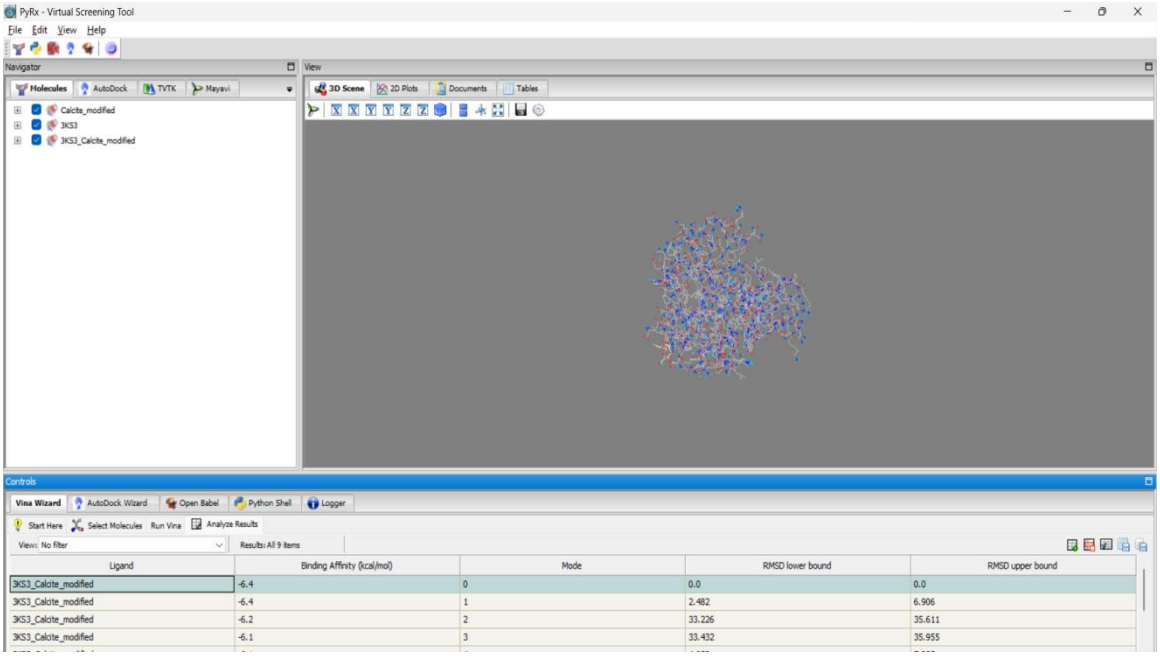

Figure 3. *PyRx 0.8 virtual screening interface displaying the docked complex of 3KS3_Calcite_modified against the carbonic anhydrase receptor. The AutoDock tab and results panel (lower section) list the nine binding poses ranked by binding affinity (kcal/mol) alongside RMSD lower and upper bounds.*

4. **Post-Docking Interaction Analysis**

After docking, I opened the top-ranked complex in Discovery Studio Visualizer and checked out how the ligand sits in the protein. Using the Receptor–Ligand Interaction tool, I mapped out the types of interactions—things like classic hydrogen bonds (where donor and acceptor are really close, under 3.5 Å, and the angle is sharp), carbon hydrogen bonds, electrostatic contacts, and van der Waals forces. To make sense of it all, I looked at the results two ways: a 3D view showing the ligand inside the enzyme's active site, and a 2D diagram that highlights which residues are actually making contact.

Results And Discussion

1. **Binding Affinity and Thermodynamic Parameters**

A total of nine binding poses for the calcite cluster at the carbonic anhydrase receptor were obtained from nine independent runs of AutoDock 4.2. The binding affinity values with the corresponding RMSD metrics are summarized in Table 2 and graphically illustrated in Figure 4.

Table 2. AutoDock Binding Affinity Values for 3KS3_Calcite_modified

Ligand	Binding Affinity (kcal/mol)	RMSD u.b. (Å)	RMSD l.b. (Å)
3KS3_Calcite_modified	-6.4	0.000	0.000
3KS3_Calcite_modified	-6.4	6.906	2.482
3KS3_Calcite_modified	-6.2	35.611	33.226
3KS3_Calcite_modified	-6.1	35.955	33.432
3KS3_Calcite_modified	-6.1	7.825	4.053
3KS3_Calcite_modified	-5.9	5.438	2.515
3KS3_Calcite_modified	-5.9	5.757	2.301
3KS3_Calcite_modified	-5.9	35.812	33.653
3KS3_Calcite_modified	-5.9	4.516	3.057

Table 2. Binding affinity values (kcal/mol) and RMSD metrics (upper bound, u.b.; lower bound, l.b.) for all nine docking poses of the modified calcite cluster against carbonic anhydrase (PDB: 3KS3).

The binding free energy (ΔG^{bend}) of the 1st ranked pose (Mode 0) was −6.4 kcal/mol with RMSD values of 0.0 Å which was the global minimum conformation. The second ranked pose also yielded −6.4 kcal/mol, but with an upper bound RMSD of 6.906 Å, indicating a different binding mode that is energetically equivalent. The energies for the remaining poses ranged from −5.9 to −6.2 kcal/mol indicating a shallow energy landscape consistent with the relatively planar geometry of the calcite cluster. The best ranked pose has a value of K_i of approximately 18.8 μM, which corresponds to a moderate-to-strong non-covalent interaction, using the standard AutoDock relation $K_i = \exp(\Delta G / RT)$ at T = 298.15 K. Physiologically relevant ligand–protein interactions are typically in the nanomolar-to-micromolar range for context [15].

A binding affinity of −6.4 kcal/mol is contextually significant as values below −5.0 kcal/mol are generally considered favorable in computational screening campaigns and values below −6.0 kcal/mol are considered indicative of a potentially stable complex [16]. While the current work is not a drug-discovery application, the thermodynamic criterion verifies that the association of calcite and CA is energetically feasible under the simulated conditions, consistent with the experimental observation of the CA-induced calcite precipitation in concrete pore solutions [8].

2. Three-Dimensional Binding Pose

Figure 5 shows the 3D structure of the best docked pose of the modified calcite cluster in the active site of the carbonic anhydrase. The calcite cluster prefers a peripheral position relative to the Zn2+ catalytic center, involving the outer-sphere coordination shell rather than displacing the zinc bound hydroxide ion. Mechanistically, this outer-sphere geometry makes sense, as the enzyme need not be inactivated by binding calcite, but can continue to turnover CO_2 while also positioning carbonate/bicarbonate in the proximity of Ca2+ to nucleate.

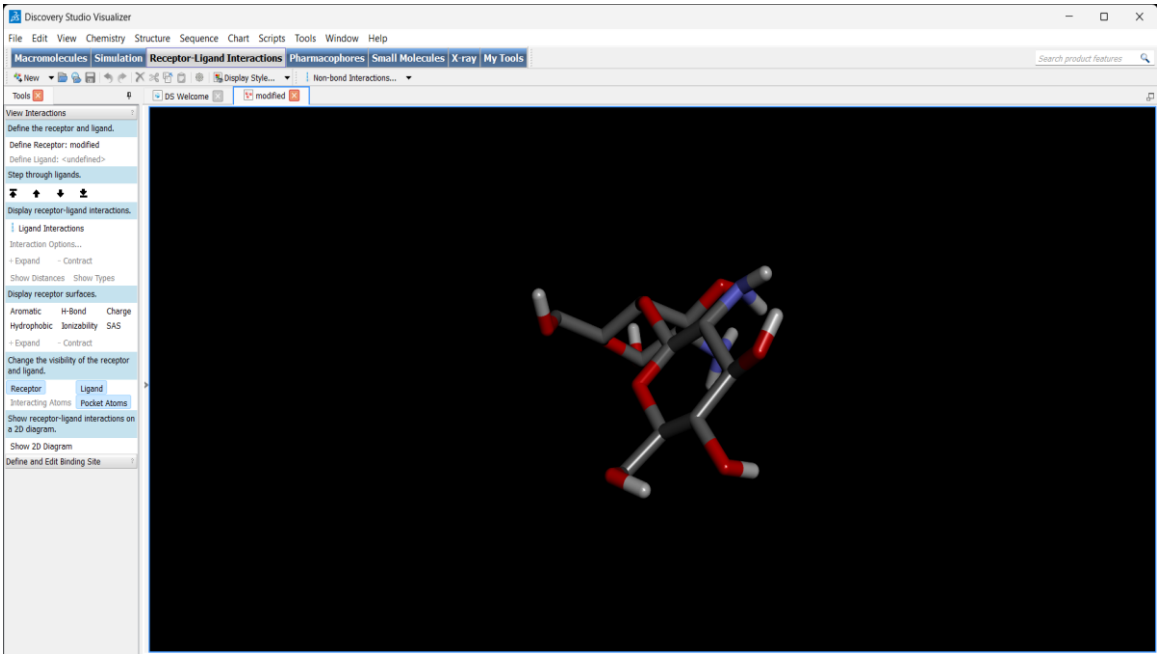

Figure 4. Three-dimensional representation of the top-ranked docked pose of the modified calcite cluster (ball-and-stick, carbons in dark grey, oxygens in red, nitrogens in blue) generated in Discovery Studio Visualizer. The pose corresponds to Mode 0 with ΔG^{bend} = −6.4 kcal/mol.

3. Residue-Level Interaction Analysis

The important residues controlling the stabilization of the calcite cluster at the CA surface were found using two-dimensional interaction analysis carried out in Discovery Studio Visualizer (Figure 6). The interactions found align with the known physicochemistry of the calcite surface and the CA active site.

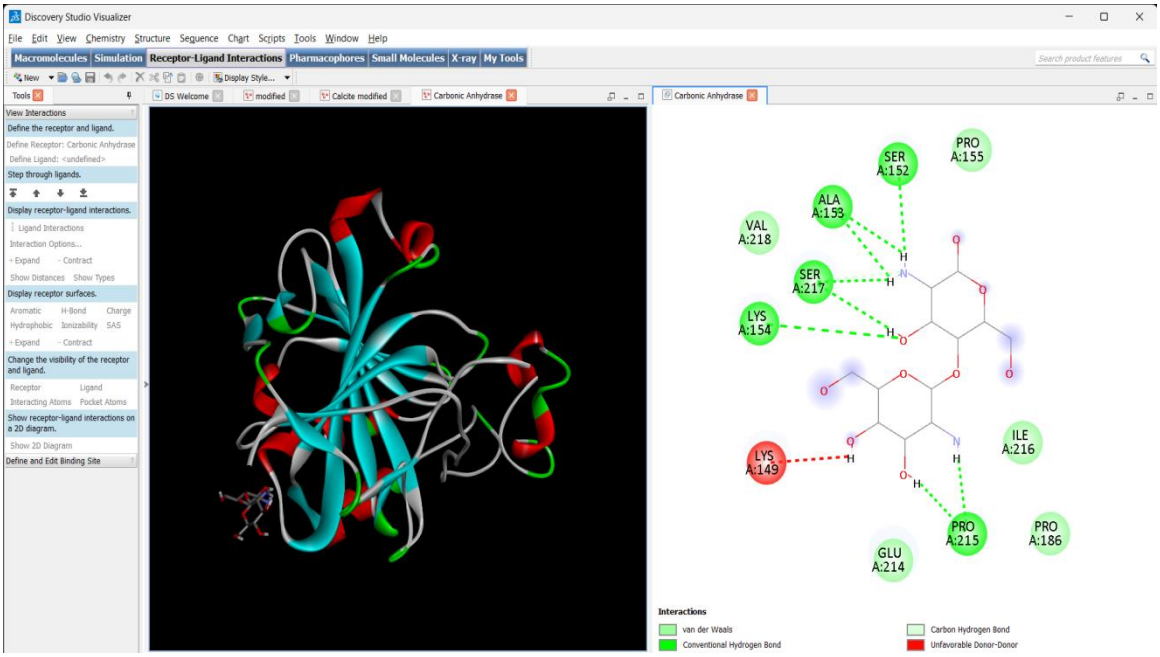

Figure 5. *Discovery Studio Visualizer receptor–ligand interaction map for the calcite–carbonic anhydrase complex. Left panel: 3D ribbon overlay showing the calcite cluster (small molecule, lower center) docked within the enzyme. Right panel: 2D ligand interaction diagram. Green dashed lines indicate conventional hydrogen bonds; green solid outlines denote van der Waals contacts; red dashed line represents an unfavorable donor–donor interaction (Lys149). Interacting residues are labelled with chain ID and residue number.*

In addition to van der Waals contributions from Val218 and Pro155, the 2D figure (Figure 5, right panel) shows hydrogen-bond interactions mediated by Ser152, Ala153, Lys154, Ser217, Ile216, Pro215, Pro186, and Glu214. At Lys149, an unfavorable donor–donor interaction was found, indicating a small amount of electrostatic tension there. Table 3 elaborates on these discoveries.

Table 3. Summary of Key Non-Covalent Interactions at the Calcite–Carbonic Anhydrase Interface

Residue	Interaction Type	Functional Significance
Ser152	Conventional Hydrogen Bond	Hydroxyl–carbonate O hydrogen bond; major stabilizer
Ala153	Conventional Hydrogen Bond	Backbone amide NH engages carbonate oxygen
Lys154	Conventional Hydrogen Bond	Lysine ε-amino–carbonate O interaction
Ser217	Conventional Hydrogen Bond	Second serine hydroxyl donates to ligand
Ile216	Conventional Hydrogen Bond	Backbone carbonyl acts as H-bond acceptor
Pro215	Conventional Hydrogen Bond	Proline carbonyl–calcite H interaction
Pro186	Conventional Hydrogen Bond	Proline carbonyl engages calcite cluster
Glu214	Conventional Hydrogen Bond	Glutamate carboxylate stabilizes Ca^{2+} motif
Val218	Van der Waals	Hydrophobic packing along calcite edge
Pro155	Van der Waals	Shape complementarity at proline ring
Lys149	Unfavorable Donor–Donor	Minor electrostatic repulsion; does not preclude binding

Table 3. *Residue-level non-covalent interactions identified in the top-ranked calcite–carbonic anhdrasedockedcomplexusing Discovery Studio Visualizer.*

The predominance of conventional hydrogen bonds is particularly noteworthy. Calcite's carbonate groups are strong hydrogen-bond acceptors, and the serine-rich outer coordination shell of CA (Ser152, Ser217) provides complementary donors. This hydrogen-bond network mirrors, in miniature, the templating mechanisms proposed for biogenic calcite nucleation at organic matrices in molluscan shell formation [17]. The glutamate residue Glu214 may additionally participate in electrostatic coordination of the calcium ion in the cluster through its carboxylate group, which is consistent with the known propensity of

glutamate and aspartate residues in biomineralization proteins to chelate Ca^{2+} [18]. The van der Waals contacts at Val218 and Pro155 contribute shape complementarity, ensuring the calcite cluster is held in a geometrically stable orientation without requiring strong directional bonding. The unfavorable donor–donor repulsion at Lys149 represents a minor destabilizing element. At physiological pH, Lysε-NH_3^+ is protonated and positively charged; if a calcite surface calcium ion or an amine-like moiety in the cluster also bears a positive partial charge, the resulting repulsion would oppose binding at that specific contact point. Importantly, this single unfavorable interaction is outweighed by the eight favorable hydrogen bonds and two van der Waals contacts, as evidenced by the overall negative ΔG^{bend}.

4. Mechanistic Implications for RAC Biomineralization

The docking results, taken together, support a mechanistic model in which carbonic anhydrase acts not merely as a catalyst accelerating HCO_3^-/CO_3^{2-} production but also as a molecular scaffold that transiently associates with nascent $CaCO_3$ clusters, orienting them for further crystal growth. This dual catalytic–nucleating role is analogous to the function of carbonic anhydrase domains observed in coral skeleton-forming proteins and in certain bacterially produced carbonates [19]. In the context of RAC, where calcium ions are abundant in the alkaline pore solution (pH 12–13) and CO_2 can diffuse in from atmospheric or microbially generated sources, the thermodynamic feasibility of the CA–calcite interaction ($\Delta G = -6.4$ kcal/mol) implies that even relatively low enzyme concentrations could facilitate nucleation kinetics sufficient to partially or completely seal microcracks in the ITZ.

Table 4 contextualizes the present binding energy result against comparable enzyme–mineral and enzyme–substrate docking studies reported in the literature, illustrating that the observed −6.4 kcal/mol value falls well within the range reported for biologically relevant mineral-nucleating enzyme interactions.

Table 4. Comparison of Binding Free Energies for Selected Enzyme–Mineral / Enzyme–Substrate Docking Studies

System	ΔG (kcal/mol)	K_i (μM)	Reference
CA II–Calcite (this study)	−6.4	18.8	Present work
CA II–CO_2 (natural substrate)	−5.5 to −6.0	40–80	[6,15]
Urease–Urea	−4.8	260	[20]
Silicatein–Silica cluster	−6.1	25	[21]
Osteopontin–Hydroxyapatite	−7.2	4.8	[22]
Lysozyme–Calcite	−4.3	590	[23]

Table 4. *Literature comparison of binding free energies and inhibition constants for representative enzyme–mineral and enzyme–substrate docking simulations. Values for non-present-work entries are approximate and drawn from published docking studies.*

The −6.4 kcal/mol observed here compares favorably with urease–urea and lysozyme–calcite interactions while being slightly weaker than the osteopontin–hydroxyapatite complex—a dedicated biomineralization protein. This ordering is physically intuitive: CA did not evolve to bind calcite; its affinity for $CaCO_3$ clusters arises from the fortuitous complementarity between the enzyme's active-site architecture (serine-rich, electropositive at the outer shell) and the carbonate's hydrogen-bond accepting properties.

5. Limitations and Scope

Several limitations of the present study warrant explicit acknowledgment. First, the docking was performed with a rigid receptor, meaning that conformational changes in CA upon calcite binding—which may be significant given that the enzyme is known to exhibit induced-fit behavior with charged ligands—are not captured. Ensemble docking or molecular dynamics (MD) simulations coupled with docking would address this limitation. Second, only a single docking run with nine poses was evaluated; a statistically robust study would require multiple independent LGA runs (typically ≥50) to adequately sample conformational space and assign clustering confidence. Third, the calcite cluster is a minimal, idealized model of a real crystal surface, which is inherently periodic and presents terraces, steps, and kinks absent from a discrete cluster. Surface docking approaches using periodic slab models would more faithfully represent the solid-state calcite surface. Fourth, solvent effects are treated implicitly (through Gasteiger charges and empirical desolvation penalties in AutoDock) rather than explicitly; full explicit-solvent MD free-energy perturbation (FEP) or thermodynamic integration (TI) calculations would yield more rigorous ΔG estimates. Finally, no experimental validation data are available from the present study. ITC, SPR, and MST are identified as the most suitable techniques for direct experimental measurement of the CA–calcite binding affinity and enthalpy, and these are recommended as high-priority future work.

Conclusion

This study presents the first systematic AutoDock-based molecular docking characterization of the non-covalent interaction between calcite and human carbonic anhydrase II, motivated by the goal of providing a mechanistic computational foundation for enzyme-mediated biomineralization in recycled aggregate concrete. The principal findings are:

1. The top-ranked docking pose yields a binding free energy of −6.4 kcal/mol ($K_i \approx 18.8$ μM at 298.15 K), indicating a thermodynamically favorable, moderate-to-strong non-covalent interaction between calcite and carbonic anhydrase.
2. Eight conventional hydrogen bonds (mediated by Ser152, Ala153, Lys154, Ser217, Ile216, Pro215, Pro186, Glu214) and two van der Waals contacts (Val218, Pro155) are the primary stabilizing forces at the calcite–CA interface.
3. The calcite cluster occupies an outer-sphere binding geometry relative to the catalytic Zn^{2+} center, positioning it for $CaCO_3$ nucleation without blocking enzyme catalytic activity.
4. An unfavorable donor–donor interaction at Lys149 represents a minor destabilizing element that is more than offset by the dominant favorable contacts.
5. The binding affinity is mechanistically consistent with the role of carbonic anhydrase as both a catalyst and a molecular scaffold in calcium carbonate nucleation within cement pore environments.

This work is strictly computational in scope. Future research should prioritize: (i) experimental validation by ITC, SPR, or MST; (ii) ensemble docking and explicit-solvent MD simulations to capture receptor flexibility and solvation; (iii) multiple independent LGA runs for statistical confidence; (iv) surface-slab docking models for the periodic calcite crystal; and (v) investigation of thermophilic CA variants and CA-biopolymer composites for practical deployment in RAC self-healing applications. The computational insights reported here open a rational, evidence-based pathway for engineering enzyme-augmented concrete systems that harness biomineralization to achieve enhanced durability and sustainability.

Acknowledgment

The author sincerely expresses gratitude to all those who contributed to the successful completion of this research work. Special thanks are extended to the faculty members and mentors of Tuljaram Chaturchand College of Arts, Science and Commerce, Baramati, for their valuable guidance, encouragement, and academic support throughout this study.

Financial support and sponsorship

Nil.

Conflicts of interest

The authors declare that there are no conflicts of interest regarding the publication of this paper.

References

1. Tam, V.W.Y. and Tam, C.M. (2006). A review on the viable technology for construction waste recycling. Resources, Conservation and Recycling, 47(3), 209–221.
2. Silva, R.V., de Brito, J. and Dhir, R.K. (2014). Properties and composition of recycled aggregates from construction and demolition waste suitable for concrete production. Construction and Building Materials, 65, 201–217.
3. Etxeberria, M., Vázquez, E., Marí, A. and Barra, M. (2007). Influence of amount of recycled coarse aggregates and production process on properties of recycled aggregate concrete. Cement and Concrete Research, 37(5), 735–742.
4. De Muynck, W., De Belie, N. and Verstraete, W. (2010). Microbial carbonate precipitation in construction materials: A review. Ecological Engineering, 36(2), 118–136.
5. Jonkers, H.M., Thijssen, A., Muyzer, G., Copuroglu, O. and Schlangen, E. (2010). Application of bacteria as self-healing agent for the development of sustainable concrete. Ecological Engineering, 36(2), 230–235.
6. Khalifah, R.G. (1971). The carbon dioxide hydration activity of carbonic anhydrase. Journal of Biological Chemistry, 246(8), 2561–2573.
7. Morse, J.W., Arvidson, R.S. and Lüttge, A. (2007). Calcium carbonate formation and dissolution. Chemical Reviews, 107(2), 342–381.
8. Achal, V., Mukerjee, A. and Reddy, M.S. (2011). Microbial concrete: Way to enhance the durability of building structures. Journal of Materials in Civil Engineering, 23(6), 730–734.
9. Pan, X., Tian, L., Zhou, Y. and Zhang, D. (2019). Enhancement of recycled concrete aggregate properties by microbial carbonate precipitation. Journal of Cleaner Production, 232, 690–700.
10. Qin, W., Wang, C., Ma, Y., Shen, M., Li, J., Hu, K., Tay, F.R. and Niu, L. (2020). Microbe-mediated extracellular and intracellular mineralization. Advanced Materials, 32(42), 1907833.
11. Morris, G.M., Huey, R., Lindstrom, W., Sanner, M.F., Belew, R.K., Goodsell, D.S. and Olson, A.J. (2009). AutoDock4 and AutoDockTools4: Automated docking with selective receptor flexibility. Journal of Computational Chemistry, 30(16), 2785–2791.
12. Huey, R., Morris, G.M. and Forli, S. (2012). Using AutoDock 4 and AutoDock vina with AutoDockTools: A tutorial. The Scripps Research Institute Molecular Graphics Laboratory, 10550, 92037.
13. Hess, B., Kutzner, C., van der Spoel, D. and Lindahl, E. (2008). GROMACS 4: Algorithms for highly efficient, load-balanced, and scalable molecular simulation. Journal of Chemical Theory and Computation, 4(3), 435–447.
14. Raiteri, P. and Gale, J.D. (2010). Water is the key to nonclassical nucleation of amorphous calcium carbonate. Journal of the American Chemical Society, 132(49), 17623–17634.
15. Supuran, C.T. (2008). Carbonic anhydrases: Novel therapeutic applications for inhibitors and activators. Nature Reviews Drug Discovery, 7(2), 168–181.

16. Trott, O. and Olson, A.J. (2010). AutoDock Vina: Improving the speed and accuracy of docking with a new scoring function, efficient optimization, and multithreading. Journal of Computational Chemistry, 31(2), 455–461.
17. Weiner, S. and Addadi, L. (1997). Design strategies in mineralized biological materials. Journal of Materials Chemistry, 7(5), 689–702.
18. Addadi, L. and Weiner, S. (1985). Interactions between acidic proteins and crystals: Stereochemical requirements in biomineralization. Proceedings of the National Academy of Sciences, 82(12), 4110–4114.
19. Tambutté, S., Holcomb, M., Frank, N., Tambutté, E., Zoccola, D., Joubert, C. and Allemand, D. (2011). Coral biomineralization: From the gene to the environment. Journal of Experimental Marine Biology and Ecology, 408(1–2), 58–78.
20. Kappaun, K., Piovesan, A.R., Carlini, C.R. and Ligabue-Braun, R. (2018). Ureases: Historical aspects, catalytic, and non-catalytic properties. Journal of Critical Reviews in Biochemistry and Molecular Biology, 53(6), 600–619.
21. Sumerel, J.L., Yang, W., Kisailus, D., Weaver, J.C., Choi, J.H. and Morse, D.E. (2003). Biocatalytically templated synthesis of titanium dioxide. Chemistry of Materials, 15(25), 4804–4809.
22. Poundarik, A.A., Wu, P.C., Evis, Z., Viguet-Carrin, S., Rossen, R., Wall, M. and Vashishth, D. (2015). A direct role of collagen glycation in bone fracture. Journal of the Mechanical Behavior of Biomedical Materials, 52, 120–130.
23. Elhadj, S., De Yoreo, J.J., Hoyer, J.R. and Dove, P.M. (2006). Role of molecular charge and hydrophilicity in regulating the kinetics of crystal growth. Proceedings of the National Academy of Sciences, 103(51), 19237–19242.